Available online at www.sciencedirect.com
ScienceDirect
Journal of Hazardous Materials 152 (2008) 196–203
Journal of Hazardous Materials
www.elsevier.com/locate/jhazmat

Properties of MSW fly ash–calcium sulfoaluminate cement matrix and stabilization/solidification on heavy metals

G.R. Qian [a,*], J. Shi [a], Y.L. Cao [a], Y.F. Xu [a], P.C. Chui [b]

[a] School of Environmental Engineering, Shanghai University, PR China
[b] School of Civil & Environmental Engineering, Nanyang Technological University, Singapore

Received 22 January 2007; received in revised form 26 June 2007; accepted 26 June 2007
Available online 6 July 2007

Abstract

In this paper, investigations were undertaken to formulate the properties of fly ash-calcium sulfoaluminate (CSA) cement matrix by blending MSW fly ash with CSA cement. The compressive strength, pore structure, hydration phases, and leaching behavior of Zn and Pb doped MSW fly ash–CSA cement matrices were determined by XRD, MIP, DSC, FTIR, EDX, TCLP leaching test and other experiments. The results showed that the addition of MSW fly ash to form fly ash–CSA cement matrix reduced the compressive strengths of matrices and made the pore distribution of matrices coarser, compared to that of pure CSA cement matrix. However, fly ash–CSA cement matrix could effectively immobilize high concentration of heavy metal such as lead and zinc with much lesser leaching of TCLP. Besides ettringite AFt, Friedel phase was a new hydration phase formed in the matrix. The formation of these hydration phases was responsible for huge reservoir of heavy metal stabilization by chemical fixing. Therefore, it could be postulated that MSW fly ash–CSA cement matrix was a potential new constituent of S/S matrix for high concentration of heavy metals such as Zn and Pb ions.

Keywords: MSW fly-ash; Calcium sulfoaluminate cement; Friedel phase; Heavy metals; Solidification/stabilization

1. Introduction

Large amount of MSW fly ashes was produced from municipal solid waste incineration plant every year from all over the world. MSW fly ash was classified as hazardous materials due to the presence of high heavy metals such as lead, zinc and potentially toxic dioxins. In view of environmental protection and resource conservation, reusing/recycling would be a better strategy for the solution of MSW fly ash. Possible applications of MSW fly ash had been extensively explored in civil paving materials, light aggregate, glass–ceramic and many others [1–4]. In our research, MSW fly ash-based glass–fiber-reinforced cement panel was being explored, it composed mixture of 20–30% MSW fly ash, 40–60% low alkalinity calcium sulfoaluminate (CSA) cement and 1–3% glass–fiber-reinforced.

The combination of calcium sulfoaluminate (CSA) cement with MSW fly ash had three interesting spots. Firstly, CSA cement is one kind of ettringite cements with high initial strength, fast hardening performance, high impermeability, frost and corrosion resistance, which is much better than those of ordinary Portland cement (OPC) [5,6]. Secondly, MSW fly ash belongs to the system of $CaO–CaCl_2–CaSO_4–SiO_2$, containing rich sulfur and chlorine which could easily react with calcium sulfoaluminate to form major hydration products such as ettringite and Friedel phase, constituting an ettringite–Friedel matrix [7,8]. Thirdly, the formation of ettringite–Friedel matrix would keep the CSA-MSW fly ash system with a lower alkalinity, which favored the durability of GFRC composites.

MSW fly ash usually contains higher content of easily leachable heavy metals. In China, source separation of municipal solid wastes was not well practiced. This resulted in high concentrations of heavy metals being detected in the MSW fly ash, from an incinerator receiving wastes from a well-developed electronic industry. It had been reported that ettringite cement matrices had higher affinities not only for cationic heavy metals but also for oxyanions, relying on the extensive substitution and solid-solution formation in the ettringite crystal structure because of its column and channel-like structure [9,10]. Meanwhile, ettringite

* Corresponding author.
E-mail address: grqian@shu.edu.cn (G.R. Qian).

0304-3894/$ – see front matter © 2007 Elsevier B.V. All rights reserved.
doi:10.1016/j.jhazmat.2007.06.118

Table 1
Main chemical compositions of MSW fly ash (wt.% by weight)

Chemical composition	(wt.%)
Na_2O	4.82
MgO	1.83
Al_2O_3	3.10
SiO_2	5.44
P_2O_5	1.62
SO_3	12.73
Cl	20.11
K_2O	4.31
CaO	42.55
TiO_2	0.92
Fe_2O_3	1.69
CuO	0.13
ZnO	1.17
Br	0.39
SnO_2	0.33
Sb_2O_3	0.15
BaO	0.15
PbO	0.42

cement matrices had a lower pore solution environment around pH 10–11. Conner postulated that amphoteric heavy metals will keep insoluble with a stable precipitation in a lower alkaline pore solution environment [11]. Additionally, Friedel phase is also a member of hydroculmite family assembly with the layered structure [9,12,13]. It exhibited strong ions exchange capacities for heavy metals. Therefore, high solidification/stabilization potential on heavy metals from MSW fly ash by ettringite–Friedel matrix was expected.

The purpose of this work was to explore the effect of MSW fly ash addition on the properties of blend ettringite cement and the fixing abilities of novel Friedel–ettringite matrix on high concentrations of heavy metals lead and Zinc.

2. Experimental

2.1. Raw materials and preparation

Considering the fact that the compositions of MSW fly ash depends on the combustion process, seasonal and regional variations within the country, the content of heavy metals in the ash may vary significantly from one city to another. The MSW fly ash was collected from Singapore Senoko Incineration Plant and its chemical compositions was given in Table 1. The particle size of the fly ash used in the following experiments was finer than 0.64 mm. The chemical compositions of OPC cement and CSA cement were given in Table 2.

Table 3
Mix proportions of designed matrices (%)

	OPC	CSA	MF	Pb	ZN
F0		70	30		
OPC–Pb	100			2	
EP		100		2	
FP1		70	30	0.1	
FP2		70	30	0.5	
FP3		70	30	2	
OPC–ZN	100				2
EZ		100			2
FZ1		70	30		0.1
FZ2		70	30		0.5
FZ3		70	30		2

OPC: ordinary Portland cement, CSA: calcium sulfoaluminate cement, MF: MSW incineration fly ash.

The samples in the tests were classified according to three series: (1) OPC series, denoted as OPC–Pb and OPC–Zn, they were prepared with 100% ordinary Portland cement mixed with 2% Pb and Zn ions, respectively; (2) E series, denoted as EP and EZ, it was prepared with 100% CSA cement mixed with 2% Pb and Zn ions, respectively; (3) F series, denoted as FP and FZ, they were prepared with 70% CSA cement and 30% MSW fly ash, mixed with 0, 0.1, 0.5 and 2% Pb and Zn ions, respectively. In our work, the first OPC series and the second E series were used as the reference. The third F series represented novel MSW fly ash–CSA cement matrices, among which blank matrix F0 without addition of Pb and Zn ions was designed in order to test the role of novel MSW fly ash–CSA cement matrices in fixing heavy metals from itself MSW fly ash. Detailed information of mixtures could be seen in Table 3. Chemically pure $Pb(NO_3)_2{\cdot}6H_2O$ and $Zn(NO_3)_2{\cdot}6H_2O$ were initially dissolved in water and then mixed with matrices. All the pastes of the solidification matrix were prepared at a water to cement ratio of 0.30.

These pastes were mixed in a standard laboratory mixer, casted into molds of ISO 50 mm × 50 mm cubes and shaken in a laboratory shaker. All the samples were first matured with 95% humidity in the molds for 24 h at 20 °C, then demoulded and cured for 1, 3, 7 and 28 days respectively.

2.2. Compressive strength test

After the specimens were cured for 1, 3, 7 and 28 days respectively, compressive strengths were tested using the unconfined compression machine with a maximum load of 5 kN. The loading rate of the machine was 1.52 m/min.

Table 2
Main chemical compositions of OPC and calcium sulfoaluminate (CSA) cement (wt.% by weight)

Formula	CaO	SiO_2	Al_2O_3	Fe_2O_3	K_2O	Na_2O	MgO	SO_3	Cl^-	Loss
OPC	67.13	20.07	4.42	2.83	1.41	n.d.	1.19	2.07	0.01	1.32
CSA	45.25	10.96	29.93	3.01	1.02	0.23	1.45	8.88	0.01	0.09

OPC: ordinary Portland cement, CSA: calcium sulfoaluminate cement.

2.3. Leaching test

The leaching test was conducted according to US EPA SW-846 TCLP test method 1311 to evaluate the leaching behaviour of Pb^{2+} and Zn^{2+} ions in the stabilized matrices. After the compressive strength test, coarse particles were separated through the use of a 9.5 mm sieve. Fifty grams of particle samples were weighed into a 1000 ml polypropylene plastic bottle containing 1000 ml of dilute acetic acid (pH 2.85) solution. The suspension was shaken for 18 h on an end-over-end shaker at the speed of 30 rpm before the suspension was filtered. The metals ions concentrations were detected by inductively coupled plasma emission spectrometer (ICP-OES).

2.4. Characterization of hydration products

After the strength tests, the specimens were crushed into coarse particles or powders and treated with acetone–alcohol solution to prevent hydration. X-ray diffraction (XRD) analysis, differential scanning calorimetry (DSC), Fourier-transform infrared spectroscopy (FTIR), and Mercury intrusion porosimetry (MIP) methods were used for identifying the hydration products. The XRD method was in Dmax/RB diffract meter from Rigaku Co. with Cu Kα radiation of 34 kV and 20 mA. The FTIR spectra were recorded using a Perkin–Elmer 1725X IR Fourier transform spectrophotometer. The spectral measurement in the 400–4000 cm^{-1} region was made at 4 cm^{-1} resolution with the use of 120 scans. DSC experiments were performed in a DSC-2920 from TA Instruments coupled with a TA-2000 control system. All the samples were heated with a rate of 10 ± 0.01 °C/min. Micromeritics Autopore III 9400 porosimeter was utilized to determine the pore size distribution of matrices.

To verify the fixation of lead and zinc in the Friedel phase, the absorption and ion exchange properties of pure Friedel phase on the lead and zinc ions in the solution, with pH 10 and 100 ppm concentration of metal ions, were detected respectively. The powder sample of pure Friedel phase adsorbed with heavy metals was examined by Energy Dispersive X-ray spectrometer (EDX) (JED-2300), at an acceleration voltage of 30 keV.

3. Results and discussion

3.1. Compressive strength

The compressive strength developments of Pb and Zn-doped fly ash–CSA cement matrices were illustrated in Fig. 1.

OPC–Pb had the highest compressive strength of 41.3 MPa at 3 days and 81.4 MPa at 28 days. Pb-doped CSA cement matrix EP displayed a good early strength of 40 MPa at 1 day, the same as that of OPC–Pb at 3 days. As MSW fly ash was combined with CSA cement, the blank matrix F0 had a slighter deduction of compressive strength at 1 day and a more significant reduction at 28 days than the matrix EP. When additional lead ions were introduced into fly ash–CSA cement matrices, the matrices FP gave 21–26 MPa at 1 day, 61–76% of blank matrix F0, 29–34 MPa at 28 days, 74–87 of blank matrix F0. It suggested that Pb ions will significantly reduce the compressive strength of fly ash–CSA cement matrix. However, it was noticed that the strength for FP3 with 2% Pb approximated to that of blank matrix F0 after hydrated for 28 days.

The compressive strengths of Zn-doped cement matrices and Pb-doped cement matrices had remarkable differences. Zinc had a highly depressive effect on early compressive strength of OPC–Zn matrix. It only gave 2.3 MPa at 3 days and quickly increased to 62 MPa at 28 days. Compared to OPC–Zn, the CSA matrix EZ had a quite good early strength, of 30 MPa even at 1 day and 47 MPa at 3 days. As it was hydrated for 28 days, the matrix EZ produced the same strength of 59.8 MPa as OPC–Zn.

The effects of Zn ions on the compressive strength of fly ash–CSA cement matrices were dependent on the dosage of Zn ions. Taking blank matrix F0 as a reference, the early strength at 1 day significantly declined with the increase of Zn ions dosage.

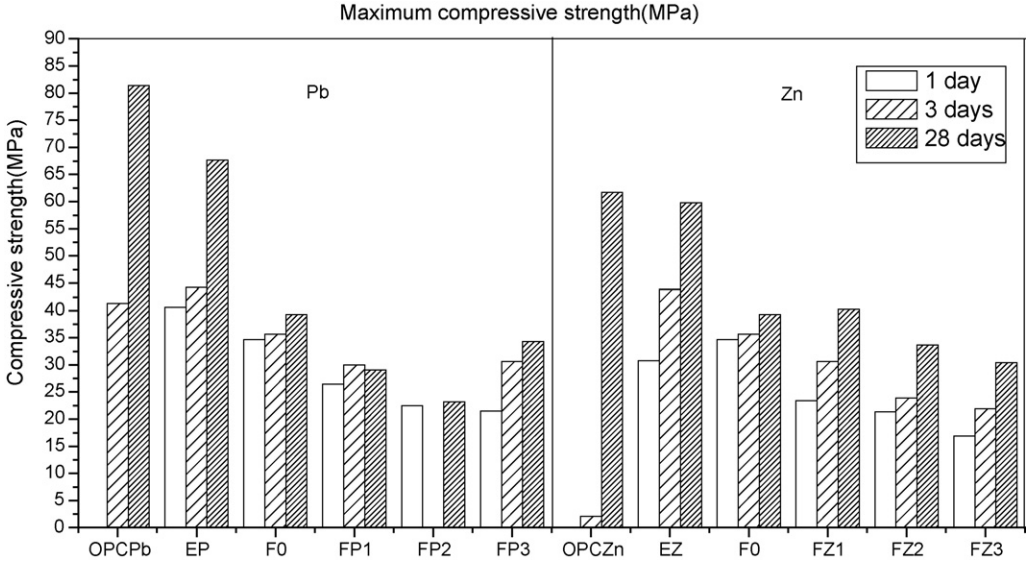

Fig. 1. Compressive strength of matrices doped with Pb and Zn ions.

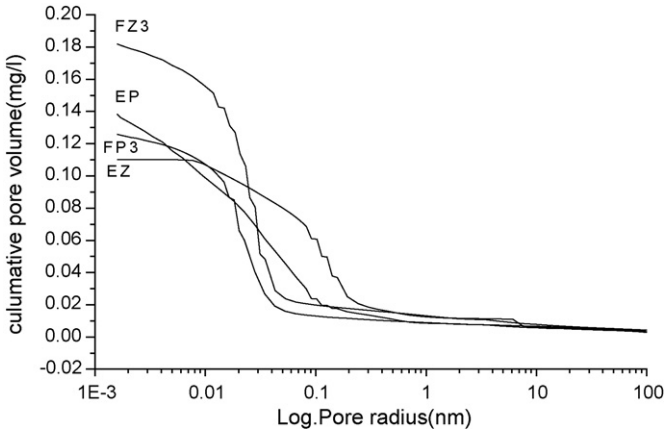

Fig. 2. Cumulative pore size distributions of matrices.

Table 4
pH value of leachates after TCLP for Pb- and Zn-doped fly ash–CSA cement matrices

pH	1 day	3 day	7 day	28 day
OPC–Pb	12.76	12.66		12.65
EP	8.38	8.29	6.73	6.73
F0	7.80	8.20	7.30	7.90
FP1	9.03	7.61	8.8	7.20
FP2	8.95	8.32	8.71	7.93
FP3	7.51	6.45	8.54	7.2
OPC–Zn	12.47	12.45		12.61
EZ	7.45	7.45	7.09	6.67
FZ1	7.70	6.59	7.28	7.70
FZ2	7.89	8.05	8.14	7.20
FZ3	7.97	8.98	7.72	6.95

The compressive strengths of FZ3 with 2% Zn ions were only 16.9 MPa at 1 day, 50% of blank matrix F0. Although this decline case of compressive strength occurred, the early strengths for Zn-doped fly ash–CSA cement matrices were much higher than for Zn-doped OPC matrix. It suggested that both CSA cement and fly ash–CSA cement had an advantage of improving the early strength of matrices induced by ZnO doping. It was also observed that the compressive strengths of FZ3 with 2% Zn ions increased to 30.1 MPa at 28 day, 80% of blank matrix F0.

3.2. Pore size distribution

The total porosity is an important indicator for evaluating the mechanical properties and leaching potential of solidification matrices. Fig. 2 shows the cumulative pore size distributions of 2% heavy metals-doped MSW fly ash–CSA cement matrices and comparison with the reference matrices for 2% heavy metals-doped pure CSA cement matrix, which were cured for 28 days. As shown in Fig. 2, 2% Pb-doped pure CSA cement matrix EP had a pore volume of 0.14 ml/g, while the replacement of calcium sulfoaluminate (CSA) cement by 30% MSW fly ash decreased the cumulative pore volume to 0.12 ml/g. The cumulative pore volume of Zn-doped CSA cement matrix was 0.11 ml/g, but that of the matrix FZ3 with 30% MSW fly ash was as high as 0.18 ml/g. Obviously, too much zinc ions could make the cumulative pore volume of MSW fly ash–CSA cement matrices significantly larger.

It was also noticed from Fig. 2 that the pore size distributions of MSW fly ash–CSA cement matrices shifted toward larger pores as MSW fly ash were added into CSA matrices. This implied that the average pore diameter became coarser due to MSW fly ash additions.

3.3. Heavy metals leachability

According to US EPA TCLP guideline, the allowable regulatory limit for Pb is below 5 mg/l, while the regulatory limit for Zn is not available. The cumulative amounts of heavy metal ions released in the leaching test with acetic acid (pH 2.85) solution are reported in Fig. 3. The pH values after TCLP test are presented in Table 4. For pure ordinary Portland cement matrices with 2% Pb addition, all the leachings of Pb^{2+} ions from OPC–Pb

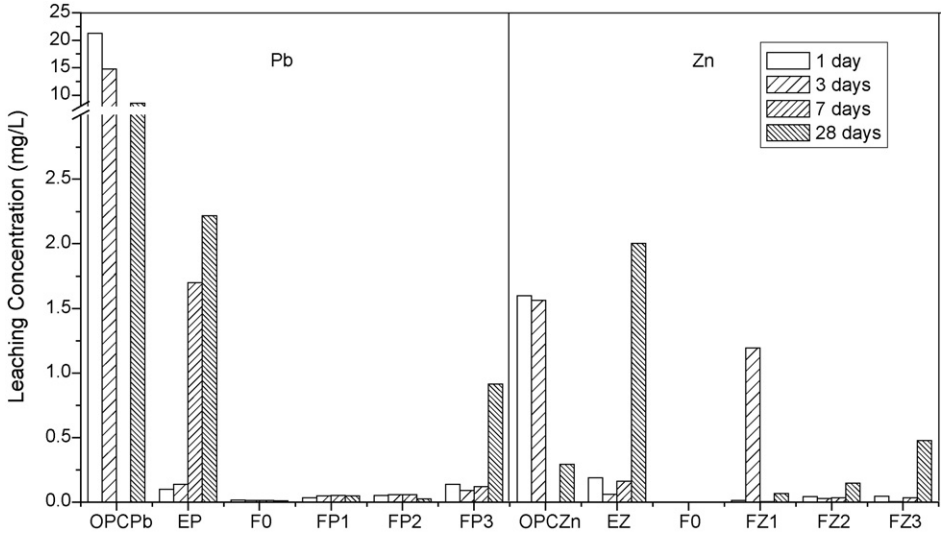

Fig. 3. Leaching from Pb- and Zn-doped fly ash–CSA cement matrices.

matrices were quite excessive, 21.26 mg/l at 1 day, 14.75 mg/l at 3 day and 8.54 mg/l at 28 day, exceeding the TCLP limit by US-EPA. As shown in Table 3, the pH of TCLP leachate was between 12.5 and 12.7. As lead is an amphoteric heavy metal, a highly alkaline aqueous environment would make lead to be easily leached from the matrix.

Compared with pure OPC–Pb matrices, as shown in Fig. 3, the Pb^{2+} leaching results of EP series matrices were below 5 mg/l level, the maximum Pb level given in the TCLP guidelines. Due to rapid hydration, the leaching from matrices was quite low even in the early hydration age of 1 day. The leaching from EP with 2% Pb, cured for 1 day, was only 0.098 mg/l, far less than that from OPC–Pb matrix.

MSW fly ash is classified as hazardous waste because of heavy metals and dioxin. From the chemical compositions of MSW fly ash shown in Table 1, it contained 1.17% ZnO and 0.42% PbO. While only MSW fly ash was tested by TCLP method, 40–60 mg/l Pb and 20–30 mg/l Zn could be detected due to the leaching, related with its chemical speciation fractions with easily exchangeable and acid soluble [14]. However, the blank matrix F0 with 70% CSA cement and 30% MSW fly ash had neglectable leaching of all heavy metals at all hydration ages, only several ppb or less detected.

As additional Pb ions were added into MSW fly ash–CSA cement matrices, it was interestingly noticed that novel FP matrices had a much more depressed leaching of Pb^{2+} than that of pure CSA matrices. For all the hydration ages, the leaching of Pb^{2+} from matrices of both FP1 and FP2 approximated to zero. Although the leaching from FP3 with 2% Pb was slightly higher than the others, it was apparently lower than EP, especially at 7 and 28 days.

Regarding the leaching of Zn^{2+} ions from the matrices, the results from matrices EZ were 0.188 mg/l at 1 day, 0.059 mg/l at 3 day, 0.161 mg/l at 7 day and 2.001 mg/l at 28 day. However, it was noticed that nearly all the leaching of Zn^{2+} ions from fly ash–CSA matrices FZ, except for two data, were quite little, only several dozen ppb, similar to that from the leaching of Pb^{2+} ions. Especially at curing of 1 day, this effective fixation of fly ash–CSA matrices on Zn^{2+} ions just appeared.

Based on the results in Fig. 3, it could be observed that fly ash–CSA matrices demonstrated the least leaching of Pb^{2+} and Zn^{2+} among the OPC, E and F matrices, as the same concentration of heavy metal ions were combined into different S/S matrices. Judging by the compressive strengths (Fig. 1) and pore distributions of matrices (Fig. 2), however, addition of MSW fly ash into CSA cement matrices would lead to the decrease of strength and increase of pore size. Therefore, physical encapsulation was not a major mechanism responsible for the fixation of high concentration of heavy metals Pb and Zn in the fly ash–CSA cement matrices.

As listed in Table 4, the final pH of leachate from OPC matrix after TCLP was about 12.5–12.7, slightly lower than the alkalinity of OPC matrix. Different from OPC matrix, CSA cement matrix and fly ash–CSA cement matrix displayed a very weak acid neutralization capacity and their final pH was only about 7–9, far less than the original alkalinity of pH 11–12. Although weak acid neutralization capacity, the final pH of 7–9 was advantageous in keeping amphoteric heavy metals less leached.

3.4. Characterization of hydration products in matrices

Based on the physical properties and the leaching behavior of heavy metals exhibited by MSW fly ash–CSA cement matrices, it was obvious that MSW fly ash was a good S/S material that effectively stabilized the high concentration of heavy metals, particularly during the early hydration ages. Physical properties and microstructures of MSW fly ash–CSA cement matrices were controlled by their hydration process and reaction products, both of which could be well characterized by XRD, DSC and FTIR methods.

3.4.1. XRD analysis

The XRD patterns of 2% Pb and Zn-doped fly ash–CSA cement matrices after hydrated for 1 day are illustrated in Fig. 4.

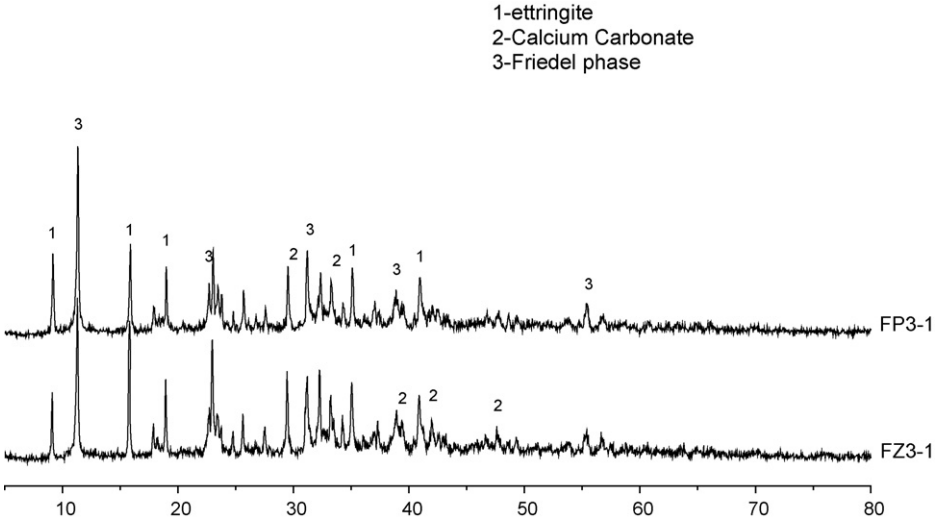

Fig. 4. XRD patterns of 2% Pb- and Zn-doped fly ash–CSA cement matrices after 1 days of hydration.

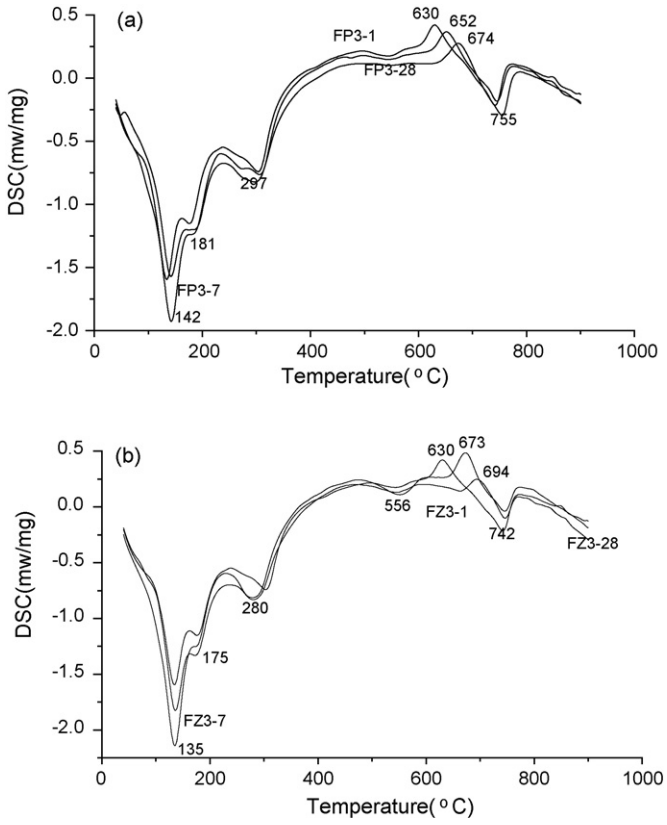

Fig. 5. DSC curves of heavy metals-doped fly ash–CSA cement matrices (a) lead and (b) zinc.

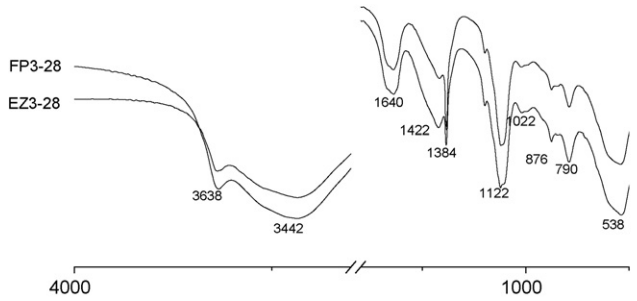

Fig. 6. FTIR patterns of Pb- and Zn-doped fly ash–CSA cement matrices after 28 days of hydration.

In the pure CSA cement matrix, there were some hydration products, such as ettringite AFt, calcium aluminum hydration products and calcium carbonate. Different from the CSA cement matrices, fly ash–CSA cement matrix formed a new hydration product Friedel phase, besides ettringite AFt and $CaCO_3$. The main peaks for ettringite AFt were at 9.68, 5.61, 3.87 and 2.78 Å in the fly ash–CSA cement matrices. The main peaks of $CaCO_3$ were at 3.03, 2.28, 2.1 and 1.91 Å. Apart from these hydration phases, a new reaction product Friedel phase peaked at 7.81, 3.91 and 2.87 Å. During the hydration of fly ash–CSA cement matrices, the formation of Friedel phase was due to the reaction of chlorine from MSW fly ash with calcium aluminum hydration products in cement.

3.4.2. DSC analysis

The presence of hydration reaction products in the fly ash–CSA cement matrix could also be characterized by DSC. Fig. 5 shows the DSC curves of 2% heavy metals-doped fly ash–CSA cement matrices cured for 1, 7 and 28, respectively. The endothermic peaks at about 142 °C for all the matrices showed the presence of ettringite [15], whereas the endothermic peaks at around 180 and 290 °C indicated the presence of Friedel phase [16]. It was also noticed that the endothermic peaks of reaction products at 180 and 290 °C after 28 days of hydration were similar to that at 1 and 3 day. It suggested that Friedel phase could be rapidly formed at 1 day. As compared to Pb-doped fly ash–CSA matrices, the feature peaks of ettringite and Friedel phases in Zn-doped fly ash–CSA matrices shifted to the lower temperatures, the consequence of different heavy metal ions fixed in the structure of ettringite and Friedel phase.

The exothermic peaks for matrices FP3-1, FP3-7 and FP3-28 at 630, 652 and 675 °C respectively were related with the recrystallization of Friedel phase, producing calcium chloroaluminate, $11CaO{\cdot}7Al_2O_3{\cdot}CaCl_2$ [11]. It was also observed in Fig. 5(b) that 2% Zn-doped fly ash–CSA cement matrices cured for 1, 7 and 28 days showed an obvious exothermic peak of DSC around 630–694 °C, which could further support the presence of Friedel phase. At around 742–755 °C, there was endothermic phenomenon of decarbonation due to the calcite present in all matrices.

3.4.3. FTIR analysis

The microstructure of hydration products could be characterized by Fourier transform infrared (FTIR) spectrum. The FTIR spectrum of Pb or Zn-doped cement matrices after 28 day of hydration are shown in Fig. 6.

The spectrum shows the absorption bands at around 3638 cm^{-1}, which could be ascribed to OH stretching vibration in the structure of ettringite AFt. The band at around 1640 cm^{-1} was an H–OH vibration (ν_2H_2O) of interlayer water for Friedel phase, whereas the broad band at 3442 cm^{-1} was due to vibration (νOH) in structural water. For pure Friedel phase, there was a very strong feature at around 786 cm^{-1} being Al-OH bending mode [13]. This band shifted to a higher frequency at 788 cm^{-1} for FZ3-28 and 790 cm^{-1} for FP3-28, which possibly meant the incursion of heavy metals in the structure of Friedel phase. Chloride does not absorb in the range 400–4000 cm^{-1}.

The band at 876 cm^{-1} represented the presence of symmetric and asymmetric vibrations of Al–OH band in $Al(OH)_6$ octahedral structure of ettringite in fly ash–CSA cement matrices. But the frequency of Al-OH band for pure ettringite AFt was at 872 cm^{-1}. This difference might be another proof of heavy metals Pb and Zn fixed in the structure of ettringite AFt phase. The FTIR band of SO_4^{2-} in ettringite AFt exhibited around 1120 cm^{-1} [17]. The other strong absorption band around 1422 cm^{-1} was attributed to the ν2 vibration of CO_3^{2-} due to carbonation [18].

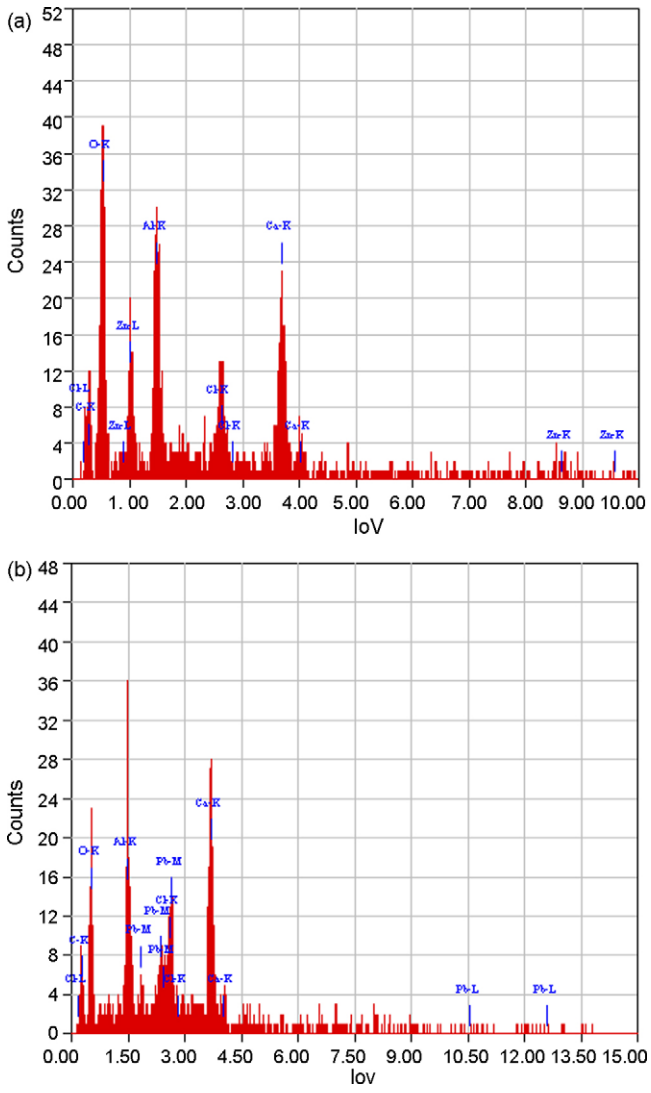

Fig. 7. EDX analyses of pure Friedel phase absorbed with heavy metals (a) zinc and (b) lead.

3.4.4. EDX analysis

To explore the fixation mechanisms of Friedel phase on Pb, Zn ions, the absorption and ion exchange behavior of pure Friedel phase on Pb, Zn ions in the solution was detected [12]. Solid particles of Friedel phase after reacted for 24 h were scanned by EDX. As shown in Fig. 7, there were visible peaks of Pb and Zn in elemental distributions of EDX, further supporting that Friedel phase could hold both Pb and Zn in its crystal structure.

In the view of crystal structure, Friedel phase assumed the laminated structure with the same family of layered monosulfur hydration calcium sulfoaluminate (AFm) [13]. Layered monosulfur hydration calcium sulfoaluminate (AFm) had a very strong ion exchange and fixing ability for the heavy metal cations Cd^{2+}, Pb^{2+}, Zn^{2+}. This exchange and fixing could be done by way of substitution and exchanges of Ca and Al in positive charge host layer of $[Ca_2Al(OH)_6]^+$ with cations [9]. The unit cell of Friedel phase consisted of two such host layers and the excess positive charges were balanced by anions Cl^- in interlayer spaces. Fig. 7 revealed that the heavy metal cations Pb and Zn could be effectively fixed in the crystal lattices of pure Friedel phase. Based on the results, it was presumed that the less leaching from FP3 or FZ3 were related with the fixation of Pb and Zn ions in the crystal lattice of Friedel and ettringite phases, which formed in MSW fly ash–CSA cement matrices.

4. Conclusions

1. The addition of MSW fly ash to form fly ash–CSA cement matrix decreased the compressive strengths of matrices while the pore distribution of matrices became coarser, compared with pure CSA cement matrix. However, MSW fly ash could improve the early strength of Zn-doped matrices, compared with Zn-doped OPC matrices.
2. The fly ash–CSA cement matrices could effectively immobilize high concentration of heavy metals such as lead and zinc. This fixation ability by fly ash–CSA cement matrices was more prominent than that by OPC matrices even at 1 day of hydration.
3. Friedel phase was a new hydration phase detected in MSW fly ash-cement matrices, besides ettringite. These hydration phases were responsible for huge reservoir of heavy metal stabilization by chemical binding.

Acknowledgements

This project is supported by National Nature Science Foundation of China No. 20477024, No. 20677037, Shanghai Leading Academic Disciplines (T105).

References

[1] C. Ferreira, A. Ribeiro, L. Ottosen, Possible applications for municipal solid waste fly ash, J. Hazard. Mater. 96 (2003) 201–216.
[2] N. Saikia, S. Kato, T. Kojima, Production of cement clinkers from municipal solid waste incineration (MSWI) fly ash, Waste Manage. 27 (2007) 1178–1189.
[3] G. Qian, Y. Song, C. Zhang, Y. Xia, H. Zhang, P. Chui, Diopside-based glass–ceramics from MSW fly ash and bottom ash, Waste Manage. 26 (2006) 1462–1467.
[4] T. Mangialardi, Sintering of MSW fly ash for reuse as a concrete aggregate, J. Hazard. Mater. 87 (2001) 225–239.
[5] J. Péra, J. Ambroise, New applications of calcium sulfoaluminate cement, Cement Concrete Res. 34 (2004) 671–676.
[6] F.P. Glasser, L. Zhang, High-performance cement matrices based on calcium sulfoaluminate–belite compositions, Cement Concrete Res. 31 (2001) 1881–1886.
[7] S. Auer, H.-J. Kuzel, H. Pöllmann, F. Sorrentino, Investigation on MSW fly ash treatment by reactive calcium aluminates and phases formed, Cement Concrete Res. 25 (1995) 1347–1359.
[8] A.K. Suryavanshi, J.D. Scantlebury, S.B. Lyon, Mechianism of Friedel's salt formation in cements rich in tri-calcium aluminate, Cement Concrete Res. 26 (1996) 717–727.
[9] M. Chrysochoou, D. Dermatas, Evaluation of ettringite and hydrocalumite formation for heavy metal immobilization: Literature review and experimental study, J. Hazard. Mater. 136 (2006) 20–33.
[10] W.A. Klemm, J.I. Bhatty, Fixation of heavy metals as oxyanion-substituted ettringites, Portland Cement Association (2002), http://www.portcement.org.
[11] J.R. Conner, Chemical Fixation and Solidification of Hazardous Wastes, Van Nostrand-Reinhold, New York, 1990.

[12] C. Yali, Fixation of Heavy Metal-Pollutants by Friedel's Salt, Master thesis, Shanghai University, Shanghai, PR China, 2006.
[13] U.A. Birnin-Yauri1, F.P. Glasser, Friedel's salt, $Ca_2Al(OH)_6(Cl,OH)\cdot 2H_2O$: its solutions and their role in chloride binding, Cement Concrete Res. 28 (1998) 1713–1723.
[14] D. Shixiang, Q. Guangren, Novel solidification/stabilization matrices for safe landfill by utilizing MSWI fly ash, Acta Scientiae Circumstantiae 25 (2005) 1052–1057.
[15] W. Sha, E.A. O'Neill, Z. Guo, Differential scanning calorimetry study of ordinary Portland cement, Cement Concrete Res. 29 (1999) 1487–1489.
[16] P. Ubbriaco, Hydration behaviour of a lime-pozzolan cement containing MSW incinerator fly ash, J. Therm. Anal. 47 (1996) 7–16.
[17] S.C.B. Myneni, S.J. Traina, G.A. Waychunas, Vibrational spectroscopy of functional group chemistry and arsenate coordination in ettringite, Geochimica Et Cosmochimica Acta, 62 (1998) 3499–3514.
[18] M.Y.A. Mollah, F. Lu, D.L. Cocke, An X-ray diffraction (XRD) and Fourier transform infrared spectroscopic (FT-IR) characterization of the speciation of arsenic (V) in Portland cement type-V, Sci. Total Environ. 224 (1998) 57–68.